Inorganic Chemistry

Communication

pubs.acs.org/IC

Non-Heme Mononitrosyldiiron Complexes: Importance of Iron Oxidation State in Controlling the Nature of the Nitrosylated Products

Amit Majumdar and Stephen J. Lippard*

Department of Chemistry, Massachusetts Institute of Technology, Cambridge, Massachusetts 02139, United States

Supporting Information

ABSTRACT: Mononitrosyldiiron complexes having either an $[Fe^{II}\cdot\{FeNO\}^7]$ or an $[Fe^{III}\cdot\{FeNO\}^7]$ core formulation have been synthesized by methods that rely on redox-state-induced differentiation of the diiron starting materials in an otherwise symmetrical dinucleating ligand environment. The synthesis, X-ray structures, Mössbauer spectroscopy, cyclic voltammetry, and dioxygen reactivity of $[Fe^{III}\cdot\{FeNO\}^7]$ are described.

Nitric oxide is a major component of the immune defense system in macrophages.[1] Although the immune system can generate micromolar concentrations of NO, many pathogenic microbes such as *Trichomonas vaginalis*,[2] *Escherichia coli*,[3,4] and *Neisseria meningitidis*[5,6] reduce NO to N_2O[7] by expressing flavodiiron nitric oxide reductases (FNORs).[8] Crystallographic studies[9−11] of these enzymes reveal active sites (*Desulfovibrio gigas*)[9] comprising two non-heme iron centers in an unsymmetrical coordination environment provided by histidine, glutamate, aspartate, and water-based ligands. The active site binds NO to generate a high-spin $\{FeNO\}^7$ species with total spin $S = {}^3/_2$.[8,11,12] Although two conflicting mechanisms involving both mono- and dinitrosyldiiron intermediate species have been proposed for this chemistry,[8,13,14] recent results favor the mononitrosyl.[11,15] These reports include formation of a stable mononitrosyl adduct, formed by addition of 1 equiv of NO per diiron(II) site of both FMN-free[10] and FMN-containing flavin diiron proteins.[15]

Reactions of NO with synthetic non-heme diiron complexes have been known for over 15 years.[13,16] The first report of a dinitrosyl compound, $[Fe_2(N\text{-Et-HPTB})(PhCOO)(NO)_2](BF_4)_2$ (**5a**),[17] where *N*-Et-HPTB is the anion of *N*,*N*,*N*′,*N*′-tetrakis[2-(1-ethylbenzimidazolyl)]-2-hydroxy-1,3-diaminopropane, was followed by the study of an analogous compound, $[Fe_2(BPMP)(OPr)(NO)_2](BPh_4)_2$ (**5b**).[18] Compounds **5a**[17] and **5b**[18] represent $\{Fe(NO)^7\}_2$ species ($S = {}^3/_2$), and **5b** could be reduced by two electrons, leading to formation of N_2O.[18] Although formation of an EPR-silent $[Fe^{III}\cdot\{FeNO\}^7]$ species was postulated during oxidation of deoxyhemerythrin to the semimet form by nitrite ion,[19] there is no report to date of any synthetic *mono*nitrosyldiiron compound coordinated by an O/N-donor dinucleating ligand system. Here we describe the synthesis and characterization of the two such compounds in this class and the importance of the iron oxidation state in controlling the nature of the resulting nitrosylated diiron products.

Compounds **5a** and **5b** were stable in solution only in the presence of excess NO gas, and formation of mononitrosyldiiron species was never observed.[17,18] We discovered, however, that with use of a mixed-valent diiron(II,III) compound to be reported in detail elsewhere, $[Fe_2(N\text{-Et-HPTB})(PhCOO)(DMF)_2](BF_4)_3$ (**2**),[20] addition of 1 equiv of tritylnitrosothiol (Ph_3CSNO) yielded a mixture of two of four crystalline forms of the compound $[Fe_2(N\text{-Et-HPTB})(NO)(OH)(DMF)_2](BF_4)_3$, **4c** and **4d** (Scheme 1). There are slight differences in the core

Scheme 1. Schematic Depiction for the Synthesis of Mononitrosyl Complexes[a]

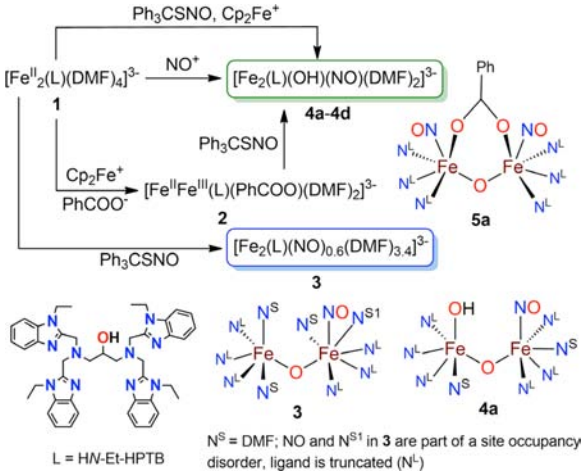

[a]Complexes **4a**−**4d** are chemically equivalent but possess different Fe−N—O angles (Table 1). Also shown are the protonated form of the ligand and immediate coordination environment of **3**, **4a**, and **5a**.

structures of **4c** and **4d** (Table 1 and Figure S1 in the Supporting Information, SI), but they are otherwise chemically identical. The product was contaminated with $[Fe_2(N\text{-Et-HPTB})(PhCOO)](BF_4)_2$ (**6**),[21] as evidenced by Mössbauer spectroscopy (Figure S2 in the SI) and by an X-ray structure determination of light-yellow crystals (**6**) found in the sample. To avoid these complications, alternative synthetic routes were explored.

A reaction system containing **6**[21] and 1 or 2 equiv of Ph_3CSNO generated a green solution, which, upon workup, afforded only the starting material **6**, as determined by IR spectroscopy and X-

Received: July 27, 2013
Published: November 18, 2013

Table 1. Selected Bond Distances, Angles, and NO Stretching Frequencies

	3	4a	4b	4c	4d
Fe−N (Å)	1.762(1)	1.787(2)	1.764(4)	1.794(4)	1.790(4)
N−O (Å)	1.118(2)	1.110(4)	1.109(6)	1.100(6)	1.147(6)
$Fe-O_L$ (Å)	2.032(3)	1.952(2)	1.951(3)	1.958(3)	1.965(3)
	2.020(3)	2.044(2)	2.048(3)	2.041(3)	2.044(3)
Fe−OH (Å)		1.832(2)	1.828(3)	1.837(3)	1.832(3)
Fe−Fe (Å)	3.678	3.621	3.630	3.622	3.615
$Fe-O_L-Fe$ (deg)	130.4(2)	130.0(1)	130.4(2)	129.8(2)	128.7(2)
Fe−N−O (deg)	157.8(1)	171.0(3)	168.5(4)	166.9(5)	174.4(5)
ν_{NO} (cm^{-1})	1772	1792	1792	1792	1804

1:[20] $Fe-O_L$ (Å) = 2.012(2) and 2.063(2); Fe−Fe (Å) = 3.716; Fe−O—Fe (deg) = 131.56(10). **2**:[20] $Fe-O_{ligand}$ (Å) = 1.929(2) and 2.047(2); Fe−Fe (Å) = 3.575; Fe−O—Fe (deg) = 128.06(10). **5a**:[17] $Fe-N_{av}$ (Å) = 1.750(1); $N-O_{av}$ (Å) = 1.154(4); Fe−N—O (deg) = 166.6(7) and 168.3 (7); ν_{NO} (cm^{-1}) = 1785. **5b**:[18] Fe−N (Å) = 1.774(2) and 1.796(3); N−O (Å) = 1.156(3) and 1.172(3); Fe−N—O (deg) = 155.4(2) and 144.7(2); ν_{NO} (cm^{-1}) = 1760.

ray crystallography. This result is consistent with the chemistry of **5a** and **5b**, from which NO slowly dissociates.[17,18] A different diiron(II) starting compound, $[Fe_2(N\text{-Et-HPTB})(DMF)_4](BF_4)_3$ (**1**),[20] was therefore employed. Reaction of 1 equiv of Ph_3CSNO with **1** yielded $[Fe_2(N\text{-Et-HPTB})(NO)_{0.6}(DMF)_{3.4}](BF_4)_3$ (**3**) in 66% yield, in which one of the two iron centers contains NO (59.7%) or DMF (40.3%), disordered in the crystal lattice. Compound **3** contains a $[Fe^{II}\{FeNO\}^7]$ site and should be regarded as a mixture of ~60% $[Fe^{II}\{FeNO\}^7]$ species and ~40% Fe^{II}_2 species. Reaction of **1** with Ph_3CSNO in the presence of the one-electron oxidant, $(Cp_2Fe)(BF_4)$, however, afforded the different mononitrosyl compound, **4a** (Figure 1), as greenish-brown crystals in 45% yield. An alternative method, reaction of **1** with $NO(BF_4)$, gave **4b** in 90% yield. This reaction may proceed by formal one-electron oxidation of **1** to yield a diiron(II,III) species that is rapidly quenched by NO generated in situ, which adds to the iron(II) center. The results of these reactions, taken together (Scheme 1), along with the previous report of dinitrosylation that occurs during reaction of diiron(II) compounds with excess NO gas,[17,18] clearly establish the crucial role of iron oxidation states within these diiron compounds in determining the nature of the nitrosylated products.

Compounds **4a**−**4d** contain the same $[Fe^{III}\cdot\{FeNO\}^7]$ center, with identical chemical formulas, $Fe_2(N\text{-Et-HPTB})(NO)(OH)(DMF)_2](BF_4)_3$, and identical electronic absorption spectra (Figure S3 in the SI). They display small to moderately different structural features that most likely arise from the variable solvent molecules trapped in the crystal lattice. Selected bond lengths, angles, and NO stretching frequencies for these $[Fe^{III}\cdot\{FeNO\}^7]$ complexes (**4a**−**4d**) and the $[Fe^{II}\cdot\{FeNO\}^7]$ complex, **3**, are collected in Table 1 (see Figure S4 in the SI for IR spectra). Relevant structural parameters and ν_{NO} for complexes **4a**−**4d** are quite similar to those reported for **5a** and **5b** (Table 1, footnote). In the preparation of **4c** and **4d**, the bridging benzoate of **2** is lost upon reaction with Ph_3CSNO, and a hydroxide ion, generated from water in the starting materials, binds terminally to the non-nitrosylated iron center. As a result of the benzoate loss, the Fe−Fe separations increase to 3.622 Å (**4c**) and 3.615 Å (**4d**), compared with 3.575 Å in **2**. The $Fe-O_{N\text{-Et-HPTB}}$ distances are distinctly different (Table 1) for the two iron centers in **4a**−**4d**, reflecting the different oxidation states of the metal in a manner similar, but not identical, to that observed for the diiron(II,III) compound, **2**.[20] The presence of short and long $Fe-O_{N\text{-Et-HPTB}}$ bond distances that are not as extreme as those in **2** (Table 1) is consistent with the $[Fe^{III}\cdot\{FeNO\}^7]$ formulation of the iron

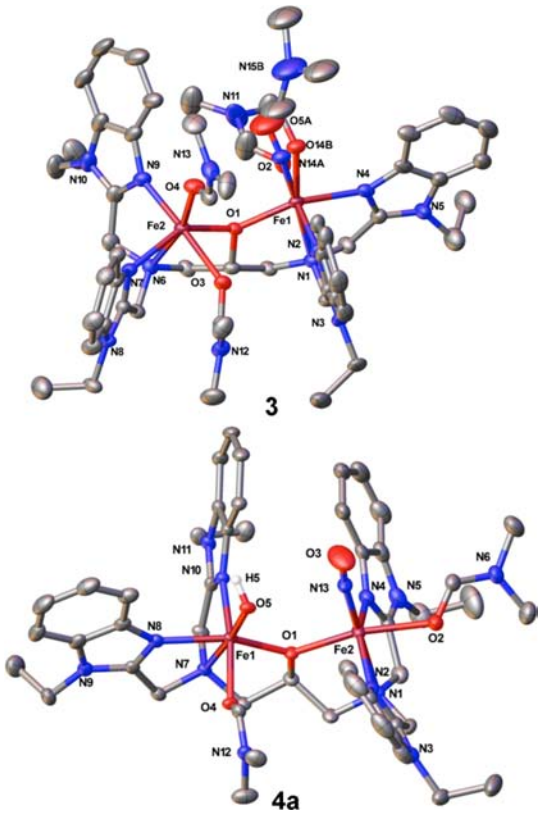

Figure 1. Molecular structures of **3** and **4a** showing 50% probability thermal ellipsoids with partial atom-labeling schemes. Hydrogen atoms are omitted (except for OH group) for clarity. Note that NO is in partial occupancy disorder with DMF at Fe1 of **3**. See Figure S1 in the SI for **4b**−**4d**.

centers in **4a**−**4d**. Mössbauer parameters obtained for **3** (Figure 2), **4a** (Figure 2), and **4b**−**4d** (Figures S2 and S5 in the SI) are very similar to those observed previously for **5a**[17] (δ = 0.67 mm/s; ΔE_Q = 1.44 mm/s), indicating the presence of a $\{Fe(NO)\}^7$ species in both **3** and **4a**−**4d**. Compound **3** should give rise to a doublet for the iron(II) site with 70% relative area and a doublet for $\{FeNO\}^7$ having 30% relative area. The observed data (Figure 2) reveal 64% iron(II) site and 36% $\{FeNO\}^7$ site, in close agreement with this prediction.

In DMF solution, compound **4a** displays two irreversible reductions (see Figure 3 and Figure S8 in the SI for

dx.doi.org/10.1021/ic4019508 | Inorg. Chem. 2013, 52, 13292−13294

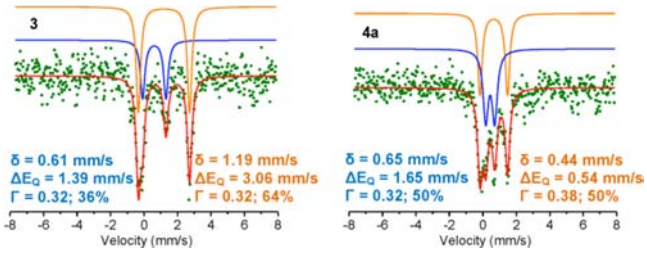

Figure 2. ^{57}Fe Mössbauer spectra for solid samples of **3** and **4a** at 77 K.

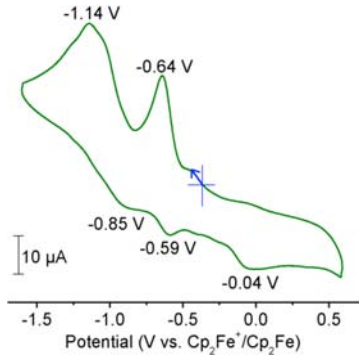

Figure 3. Cyclic voltammetric trace for **4a** in DMF. Conditions: glassy carbon working, platinum auxiliary, and silver pseudo electrodes. Scan rate = 100 mv/s; [**4a**] = 1 mM; [$(Bu_4N)(PF_6)$] = 0.1 M.

reproducibility in repeated scans); identical results were obtained for **4b**. By comparison to the presence of the irreversible, two-electron reduction in the dinitrosyldiiron compound, **5b**, at −1.1 V,[18] the reduction of **4a** at −1.14 V can be assigned to the $\{Fe(NO)\}^7$ center. The reduction at −0.64 V therefore corresponds to the $Fe^{III}(OH)$ center. Reduction of the $\{Fe(NO)\}^7$ unit in **4a** might lead to partial release of NO^- and generation of an additional iron(II) center in solution. Such behavior would possibly account for the presence of two oxidative waves on the reverse sweep (Figure 3), one at −0.59 V and the other at −0.85 V, corresponding to oxidation of $\{Fe(NO)\}^7$ and denitrosylated material. One additional feature in the cyclic voltammogram is a small oxidation at −0.04 V, which we tentatively assign to restoration of an $Fe^{III}(OH)$ unit.

In DMF solution, **4a** exhibits a broad electronic absorption spectroscopic feature centered at 600 nm (ε = 225 ± 6), a shoulder at 490 nm (ε = 377 ± 9), another weak shoulder at 420 nm (ε = 1424 ± 42), and a strong UV band at 302 nm (ε = 5910 ± 57) (Figures S3 and S6 in the SI). This solution reacts rapidly with O_2, as revealed by a change in color from light brownish-green to dark bluish-green (λ_{max} = 600 nm; ε = 725 ± 17; Figure S6a). The green solution is unstable at room temperature, and full bleaching of the 600 nm band occurs within 5 h (Figure S6b). A similar situation occurs for solutions of **4b**−**4d** (Figure S7 in the SI), consistent with their identical chemical nature. The identity of the green species is currently under investigation.

In conclusion, mononitrosyldiiron compounds having $[Fe^{III}\cdot\{FeNO\}^7]$ and $[Fe^{II}\cdot\{FeNO\}^7]$ formulations have been synthesized and characterized. The synthetic strategy used to achieve such mononitrosyl complexes relied on the presence of mixed-valent character in the initial diiron core. These results highlight the important role of iron oxidation state in controlling the nature of nitrosylation in diiron complexes with a symmetrical ligand environment. It is possible that FNORs might adopt a similar strategy to generate mononitrosyl adducts required for N_2O formation.

■ ASSOCIATED CONTENT

Supporting Information

X-ray crystallographic data for **3** and **4a**−**4d** in CIF format, structural tables, ORTEP diagrams, cyclic voltammetry, and Mössbauer, UV−vis, and IR spectroscopic data. This material is available free of charge via the Internet at http://pubs.acs.org.

■ AUTHOR INFORMATION

Corresponding Author

*E-mail: lippard@mit.edu.

Notes

The authors declare no competing financial interest.

■ ACKNOWLEDGMENTS

This work was supported by Grant GM 32114 from the National Institute of General Medical Sciences to S.J.L.

■ REFERENCES

(1) Missall, T. A.; Lodge, J. K.; McEwen, J. E. *Eukaryot. Cell* **2004**, *3*, 835−846.
(2) Sarti, P.; Fiori, P. L.; Forte, E.; Rappelli, P.; Teixeira, M.; Mastronicola, D.; Sanciu, G.; Giuffré, A.; Brunori, M. *Cell. Mol. Life Sci.* **2004**, *61*, 618−623.
(3) Gardner, A. M.; Helmick, R. A.; Gardner, P. R. *J. Biol. Chem.* **2002**, *277*, 8172−8177.
(4) Gomes, C. M.; Giuffrè, A.; Forte, E.; Vicente, J. B.; Saraiva, L. M.; Brunori, M.; Teixeira, M. *J. Biol. Chem.* **2002**, *277*, 25273−25276.
(5) Anjum, M. F.; Stevanin, T. M.; Read, R. C.; Moir, J. W. B. *J. Bacteriol.* **2002**, *184*, 2987−2993.
(6) Stevanin, T. M.; Moir, J. W. B.; Read, R. C. *Infect. Immun.* **2005**, *73*, 3322−3329.
(7) Moënne-Loccoz, P.; Fee, J. A. *Science* **2010**, *330*, 1632−1633.
(8) Kurtz, D. M., Jr. *Dalton Trans.* **2007**, 4115−4121.
(9) Frazao, C.; Silva, G.; Gomes, C. M.; Matias, P.; Coelho, R.; Sieker, L.; Macedo, S.; Liu, M. Y.; Oliveira, S.; Teixeira, M.; Xavier, A. V.; Rodrigues-Pousada, C.; Carrondo, M. A.; Le Gall, J. *Nat. Struct. Mol. Biol.* **2000**, *7*, 1041−1045.
(10) Silaghi-Dumitrescu, R.; Kurtz, D. M., Jr.; Ljungdahl, L. G.; Lanzilotta, W. N. *Biochemistry* **2005**, *44*, 6492−6501.
(11) Hayashi, T.; Caranto, J. D.; Wampler, D. A.; Kurtz, D. M., Jr.; Moënne-Loccoz, P. *Biochemistry* **2010**, *49*, 7040−7049.
(12) Brown, C. A.; Pavlosky, M. A.; Westre, T. E.; Zhang, Y.; Hedman, B.; Hodgson, K. O.; Solomon, E. I. *J. Am. Chem. Soc.* **1995**, *117*, 715−732.
(13) Berto, T. C.; Speelman, A. L.; Zheng, S.; Lehnert, N. *Coord. Chem. Rev.* **2013**, *257*, 244−259.
(14) Blomberg, L. M.; Blomberg, M. A.; Siegbahn, P. M. *J. Biol. Inorg. Chem.* **2007**, *12*, 79−89.
(15) Hayashi, T.; Caranto, J. D.; Matsumura, H.; Kurtz, D. M., Jr.; Moënne-Loccoz, P. *J. Am. Chem. Soc.* **2012**, *134*, 6878−6884.
(16) Wasser, I. M.; de Vries, S.; Moënne-Loccoz, P.; Schröder, I.; Karlin, K. D. *Chem. Rev.* **2002**, *102*, 1201−1234.
(17) Feig, A. L.; Bautista, M. T.; Lippard, S. J. *Inorg. Chem.* **1996**, *35*, 6892−6898.
(18) Zheng, S.; Berto, T. C.; Dahl, E. W.; Hoffman, M. B.; Speelman, A. L.; Lehnert, N. *J. Am. Chem. Soc.* **2013**, *135*, 4902−4905.
(19) Nocek, J. M.; Kurtz, D. M.; Pickering, R. A.; Doyle, M. P. *J. Biol. Chem.* **1984**, *259*, 12334−12338.
(20) Majumdar, A.; Apfel, U.-P.; Jiang, Y.; Moënne-Loccoz; P.; Lippard, S. J. *Inorg. Chem.* Submitted for publication.
(21) Dong, Y.; Menage, S.; Brennan, B. A.; Elgren, T. E.; Jang, H. G.; Pearce, L. L.; Que, L., Jr. *J. Am. Chem. Soc.* **1993**, *115*, 1851−1859.